Adsorption (2013) 19:1181–1187
DOI 10.1007/s10450-013-9550-3

Adsorption and desorption of toluene on nanoporous TiO_2/SiO_2 prepared by atomic layer deposition (ALD): influence of TiO_2 thin film thickness and humidity

Hyun Ook Seo · Dae Han Kim · Kwang-Dae Kim · Eun Ji Park · Chae Won Sim · Young Dok Kim

Received: 21 January 2013 / Accepted: 30 April 2013 / Published online: 9 May 2013

Abstract Adsorption and desorption of toluene on bare and TiO_2-coated silica with a mean pore size of 15 nm under dry and humid conditions were studied using toluene breakthrough curves and temperature programmed desorption (TPD) of toluene and CO_2. Two TiO_2/silica samples (either partially or fully covered with TiO_2) were prepared with 50 and 200 cycles of TiO_2 atomic layer deposition (ALD), respectively. The capacity of silica to adsorb toluene improved significantly with TiO_2-thin film coating under dry conditions. However, toluene desorption from the surface due to displacement by water was more pronounced for TiO_2-coated samples than bare samples under humid conditions. In TPD experiments, silica with a thinner TiO_2 film (50-ALD cycled) had the highest reactivity for toluene oxidation to CO_2 both in the absence and presence of water. Toluene adsorption and oxidation reactivity of silica can be controlled by modifying the silica surface with small amount of TiO_2 using ALD.

Keywords Toluene adsorption · TiO_2 · SiO_2 · Thin film · Humidity · Temperature programmed desorption (TPD)

1 Introduction

Volatile organic compounds (VOCs) are considered to be notorious pollutants indoors and are responsible for "sick-building syndrome." Much effort has been devoted to developing efficient methods to remove VOCs from air (Sinha and Suzuki 2005).

Among various methods to eliminate VOCs (e.g. catalytic oxidation, photocatalysis), adsorption of contaminants is promising. Porous materials with a high surface area, such as activated carbon (AC) (Nouri and Haghseresht 2004), metal organic framework (MOF) (Yang et al. 2011), zeolite (Pires et al. 2001), and mesoporous silica (Russo et al. 2008), have been widely used to adsorb VOCs. Many scientific studies have been performed to improve the capacity of adsorbents to adsorb VOCs and their selectivity towards specific VOCs by modifying the surface (Chiang et al. 2001; Foster et al. 1992; Li et al. 2011; Galli et al. 2010; Lee et al. 2003; Sayari et al. 2004). In our previous work, we also showed that TiO_2 thin films deposited on a nano-structured membrane (anodic aluminum oxide) by atomic layer deposition (ALD) efficiently and selectively adsorb VOCs (Lee et al. 2011).

In real applications, the effect of humidity on the capacity of an adsorption system should be considered (Vildozo et al. 2011; Ruiz et al. 1998). Previously, structure of water molecularly adsorbed on the surfaces of porous SiO_2 and TiO_2 (110) was studied. On SiO_2, water formed 3D clusters, whereas water grew in layers on TiO_2 surfaces. Also, water adsorbed more readily dissociative at structural defects, such as step and kinks (Henderson 1996; Sneh et al. 1996). Ambient water molecules have been suggested to impair selective adsorption of VOCs. Water clusters have been demonstrated to form an interfacial layer on porous adsorbents and inhibit adsorption of VOCs even at low relative humidity (RH) (Vichi et al. 2000). Water or water vapor in the gas stream can compete with VOCs for various adsorbents (Heinen et al. 2000).

After an adsorbent surface is saturated, desorption is essential to restore the adsorptive properties of a used

H. O. Seo · D. H. Kim · K.-D. Kim · E. J. Park · C. W. Sim · Y. D. Kim (✉)
Department of Chemistry, Sungkyunkwan University, Suwon 440-746, Republic of Korea
e-mail: ydkim91@skku.edu

adsorbent. Temperature-programmed desorption (TPD) techniques have been widely used to analyze the desorption behavior of adsorbed molecules (Kim and Ahn 2010; Choudhary and Mantri 2000). In addition to molecular desorption, complete oxidation of adsorbed VOCs on adsorbents, in which aromatic hydrocarbons decompose to CO_2, can take place as the desorption temperature gradually increases during TPD (Saqer et al. 2011; Everaert and Baeyens 2004; Spivey 1987). In general, total oxidation of aromatic hydrocarbons depends on the characteristics of the catalytic material. To oxidize aromatic hydrocarbons, noble metal catalysts (Liotta 2010), and metal oxide-based catalysts (Ching-Huei 2004) have been widely used, as have mixtures of noble metals and metal oxides (Tsou et al. 2005; Kim et al. 2005). Noble metals, such as Pt or Pd, have high activity and good stability at low temperatures (Papaefthimiou et al. 1999; Tidahy et al. 2007; Liotta 2010), yet they are expensive and sensitive to poisoning by chlorine (Scire et al. 2003; Liotta 2010). On the other hand, transition metal oxides or mixed oxide catalysts are inexpensive and resistant to poisoning (Saqer et al. 2011; Ching-Huei 2004; Tidahy et al. 2006).

In present work, a nano-porous TiO_2/SiO_2 catalyst was prepared by ALD to remove VOCs (Detavernier et al. 2011). Toluene adsorption behavior was studied by measuring breakthrough curves under dry and humid conditions. Complete oxidation of toluene that did not desorb at low temperature, was evaluated by measuring TPD profiles.

2 Experimental methods

2.1 Preparation of samples

TiO_2 thin films were deposited on silica gel (Sigma Aldrich, Davisil Grade 646, 35–60 mesh, pore size 15 nm) using a flow-type ALD, where two precursors (titanium tetraisopropoxide [$Ti(OCH(CH_3)_2)_4$] as a metal precursor and H_2O as an oxidizing agent) were sequentially introduced into the chamber. Before TiO_2 deposition, the silica substrate was annealed at 500 °C for 3 h in ambient conditions. Silica gel was exposed to TTIP and H_2O for 30 and 10 s at working pressures of 0.25 and 0.1 torr, respectively. TiO_2 growth by ALD is self-limiting, as only precursor molecules chemisorbed on the surface can participate in film growth. High purity N_2 (99.999 %) gas was used as the carrier and purging gas. During ALD, the base pressure was maintained below <5 mtorr. The sample was kept at 150 °C during TiO_2 deposition, the TTIP bottle was 50 °C, the water was at room temperature. After depositing TiO_2 thin film on silica, the samples were annealed at 500 °C for 3 h under atmospheric conditions.

2.2 Characterization of samples

Sample surfaces were analyzed by X-ray photoelectron spectroscopy (XPS) in an ultra-high vacuum chamber (base pressure $\sim 3 \times 10^{-10}$ torr). XPS spectra were obtained at room temperature using an Mg Kα-source (1253.6 eV) and collected in a fixed-pass-energy mode using a concentric hemispherical analyzer (CHA, PHOIBOS-Hsa3500, SPECS). The elemental composition of the sample was analyzed by inductively coupled plasma mass spectrometry (ICP-MS, Agilent 7500, Agilent). The N_2 adsorption-isotherm was used to calculate the surface area and pore size distribution by the Brunauer–Emmett–Teller (BET) method and Barett–Joyer–Halenda (BJH) plot, respectively.

2.3 Adsorption and TPD experiments

Toluene adsorption and desorption were studied in a continuous flow-type reactor under atmospheric conditions. The experimental setup comprised a linear-SUS tube (inner diameter: 4 mm, length: 30 mm, volume: ~ 250 mm^3), electric furnace, and two bottles filled with toluene and water. Each sample was closely packed into a SUS-tube. 0.3 g of the adsorbents inside the SUS-tube was pre-annealed at 300 °C for 1 h to clean the surfaces, then the sample was cooled to 30 °C. After the reactor temperature stabilized at 30 °C, toluene and water gases were injected with a carrier gas (dry air, constant flow rate of 5 ml/min). Toluene (Aldrich, purity 99.8 %) and distilled water were vaporized at 35 °C. The inlet and outlet gas concentrations were analyzed using on-line gas chromatography (GC, Agilent-6890 N) equipped with a flame ionization detector (FID). Under dry conditions, only toluene was used, whereas both toluene and water were introduced under humid conditions. The water vapor content under humid conditions was around 224 mtorr (RH 1 % at room temperature) as measured by a hygrometer. The toluene concentration was 27 ppm for both dry and humid conditions.

Toluene desorption from the sample surface was characterized by TPD where the temperature was raised from 30 to 300 °C at a rate of 1 °C/min. Before TPD, all weakly adsorbed species on the sample surface were removed by a constant flow of dry air at room temperature for 7 h. The heating rate was controlled by programmed integral–differential (PID) and electric furnace. The desorbed toluene and carbon dioxide concentrations were monitored by using a GC system.

3 Results and discussion

3.1 Characterization of samples

TiO_2/SiO_2 samples with TiO_2 thin films of different thicknesses were prepared by using different numbers of

ALD cycles (50 and 200 cycles). TiO_2 thin films deposited on silica gel by ALD were initially amorphous, while post-annealing processes (at 500 °C for 3 h) under atmospheric conditions resulted in an anatase phase of TiO_2, which was confirmed by XRD (Lee et al. 2011).

In Fig. 1, Ti 2p and Si 2p core-level XPS spectra of 2 TiO_2/SiO_2 samples (prepared with 50 and 200 ALD cycles) are displayed. An increased Ti 2p peak intensity was observed with increasing ALD cycles (from 50 to 200), while the Si 2p intensity decreased and almost disappeared after 200 ALD cycles.

ICP-Ms data demonstrated that the TiO_2/SiO_2 sample from 50 ALD cycles had Ti and Si with a ratio of 6:1. This result indicates that TiO_2 was not only deposited on the surface of silica particles but also inside deeper part of the mesoporous silica. TiO_2 islands formed on the surface, especially in the initial stage of TiO_2 deposition, i.e., during the initial stage, second and third layers of TiO_2 grew before substrate surface was completely covered by the first layer of TiO_2 (Dey et al. 2011). The FWHM of the Ti 2p core-level XPS peak from 50-ALD cycle sample was larger than that from the 200-ALD cycle sample due to a lower-binding-energy shoulder, which could be attributed to defective TiO_x in lower oxidation states (e.g. kinks, steps, or Ti–Si interfaces at the edge of TiO_2 islands). In the case 200-ALD cycle sample, however, all silica surfaces were fully covered with TiO_2 films, as indicated by the disappearance of the Si 2p peak in the XPS spectra. Considering the surface sensitivity of XPS (only the top 4–5 nm can be analyzed), the TiO_2 thickness on 200-ALD cycle samples was estimated to be higher than ~5 nm.

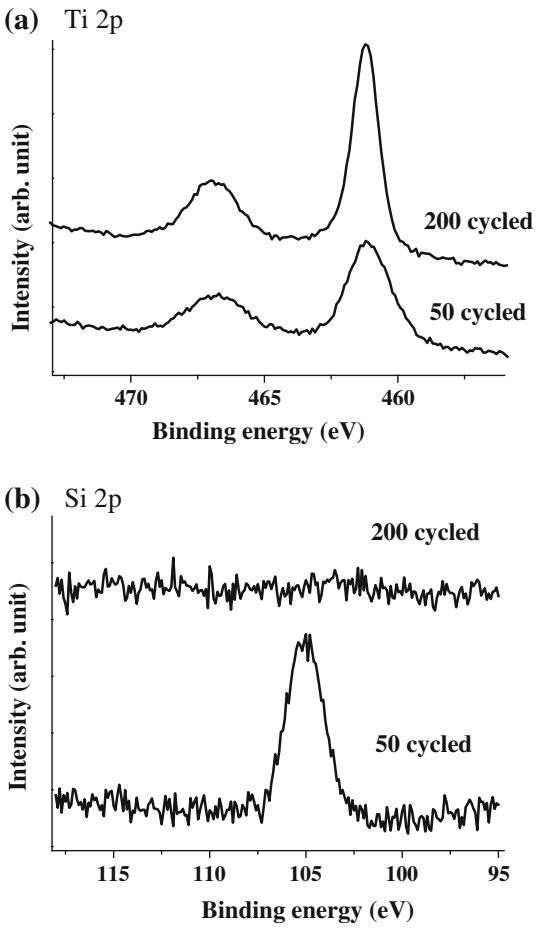

Fig. 1 **a** Ti 2p and **b** Si 2p core-level XPS spectra of 2 TiO_2/SiO_2 samples prepared with 50 and 200 ALD cycles

Table 1 BET surface area and BJH average pore size of each sample are summarized

	Surface area (m^2/g)	Pore size (nm)
Bare silica gel	312.39	13.67
TiO2/silica gel 50 cycled	289.56	11.97
TiO2/silica gel 200 cycled	272.47	11.94

Before BET measurements, all three samples were annealed at 500 °C for 3 h

Table 1 shows BET surface areas and average pore sizes of bare and TiO_2-covered silica samples (50- and 200-ALD cycle samples). Both BET surface area (m^2/g) and mean pore diameter (nm) slightly decreased as the number of ALD cycles increased; however, highly porous silica structure could be maintained after TiO_2 deposition.

Ideally, when deposition rate of TiO_2 films is the same inside and on top of smaller pores of silica, pore size should drastically decrease with increasing ALD cycles. The BET surface area and mean pore diameter of TiO_2/silica samples remained somewhat constant after depositing a large amount of TiO_2. It is notable that larger pores almost disappeared after 50 cycles deposition of TiO_2, whereas smaller pores mostly survived. The porous structure remained to some degree even after 500 ALD cycles (pore size: 11.37 nm, surface area: 268.64 m^2/g). Larger pores seem to be more selectively filled with TiO_2. A possible mechanism of TiO_2 deposition on porous silica substrate is described in Fig. 2a. TiO_2 film growth rate inside smaller pores is lower than that outside pores due to limited precursor molecule diffusion into the smaller pores (<15 nm), which maintains the porous silica substrate structure. Although this model may be too simple, it suggests that TiO_2 growth on mesoporous silica is not homogeneous, resulting in high porosity even after TiO_2 deposition.

3.2 Adsorption experiment

The toluene adsorption capacities of 3 samples (bare silica and 50- and 200-ALD cycle samples) were investigated by measuring toluene breakthrough curves under dry (Fig. 3a) and humid conditions (Fig. 3b). The differences in toluene

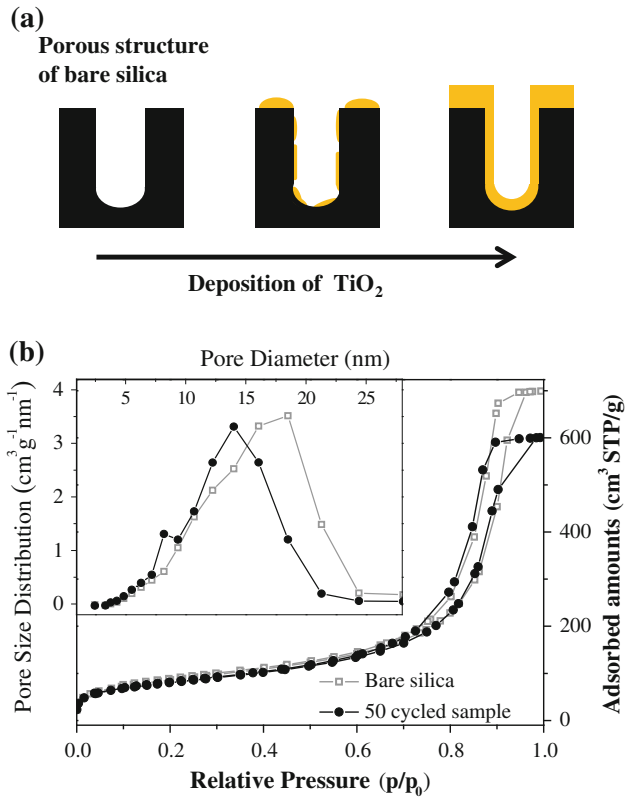

Fig. 2 **a** A schematic description of TiO_2 deposition on porous silica. **b** Nitrogen adsorption and desorption isotherms for bare silica and 50-cycle samples are shown with their pore size distribution curves

concentrations at the outlet (denoted as C_{out} in Fig. 3) and inlet (denoted as C_{in} in Fig. 3) for all 3 samples were plotted as a function of reaction time. Under dry conditions (Fig. 3a), the curves for all 3 samples had similar shapes. The breakthrough time, however, was increased gradually with increasing ALD cycles (Fig. 3a; Table 2), indicating that the TiO_2 coating improved the adsorption capacity despite the reducing the surface area and pore size (Table 1). This result implies that the TiO_2 surface had higher affinity towards toluene than the SiO_2 surface.

Adsorption capacities of the 3 samples (bare silica and 50- and 200-ALD cycle samples) under dry conditions were compared by calculating the amount of toluene adsorbed by using the following equation.

$$q = \frac{F \times C_{in}}{W}\left(T_s - \int_0^{T_s} \frac{C_{out}}{C_{in}} dt\right)$$

where q is the amount of adsorbed toluene (mg/g); F is the flow rate (ml/min); C_{in} and C_{out} are the toluene concentrations at the inlet and outlet (ppm, mg/l), respectively; T_s is the saturation time (min); and W is the sample mass (g) (Kim and Ahn 2010). Table 2 lists the calculated amounts of toluene (q) adsorbed on each sample surface with saturation time (T_s) and the breakthrough time for each case in Fig. 3a.

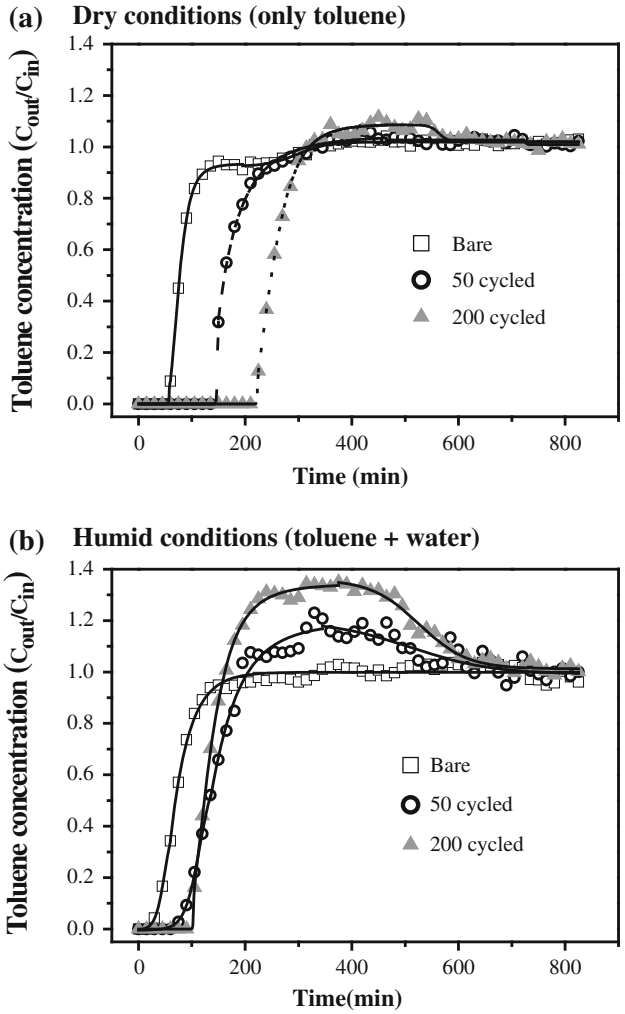

Fig. 3 Breakthrough curves of toluene for 3 bare silica and 50- and 200-cycle samples under **a** dry and **b** humid conditions

To investigate the effect of humidity on the toluene adsorption capacity of all three samples, the breakthrough curves for toluene were measured in the presence of water vapor (100 ppm). The humidity was determined by using hygrometer.

As shown in Fig. 3a, b, the adsorption behaviors of toluene on all three samples changed under humid conditions. For bare silica, water vapor decreased the breakthrough time without changing the shape of the breakthrough curve. In contrast, for TiO_2-coated samples, water vapor changed both the breakthrough times and curves. These samples had a roll-up phenomenon in each breakthrough curve, i.e., the outlet toluene concentration was temporarily higher than the inlet concentration before saturation. The roll-up phenomenon is evidence for competitive adsorption between toluene and water because the roll-up indicates that a weaker adsorbing species (toluene) is being displaced by a slower diffusing species with a

Table 2 Breakthrough time (when $C_{out}/C_{in} = 0.1$), saturation time (when $C_{out}/C_{in} = 1$), and amount of adsorbed toluene (q, mg/g) on each sample surface under dry and humid conditions in Fig. 3

Sample	Breakthrough time (min)	Ts (min)	q (mg/g)
Dry conditions			
Bare silica gel	61.47	330	132.49
TiO2/silica gel (50 cycled)	139.38	330	203.16
TiO2/silica gel (200 cycled)	222.21	315	277.28
Humid conditions			
Bare silica gel	36.49	330	114.93
TiO2/silica gel (50 cycled)	91.21	540	107.36
TiO2/silica gel (200 cycled)	99.0	690	10.88

stronger affinity (water) (Heinen et al. 2000; Avila and Breiter 2008). The water tended to grow in layers on the TiO_2 surface, i.e., a first layer of water molecules completely covers the TiO_2 surface before a second layer grows, whereas water formed 3D clusters on the porous silica surface (Henderson 1996; Sneh et al. 1996). This result shows that TiO_2 has a higher affinity towards water molecules, and toluene adsorption sites on a TiO_2 surface were blocked by water molecules more efficiently than sites on the SiO_2 surface, resulting in roll-up curves with increasing TiO_2 deposition.

3.3 Temperature-programmed desorption (TPD)

Toluene desorption from bare and TiO_2-deposited silica samples were studied using toluene and CO_2 TPD analysis. After measuring toluene breakthrough curves, weakly adsorbed toluene molecules were removed from each sample at 30 °C for 7 h under the flow of dry air. Then, the temperature was raised from 30 to 300 °C at a constant rate of 1 °C/min to obtain TPD curves. In Fig. 4, the normalized toluene (Fig. 4a, b) and CO_2 concentrations (Fig. 4c, d) were plotted as a function of desorption temperature. No desorption species other than toluene and CO_2 were

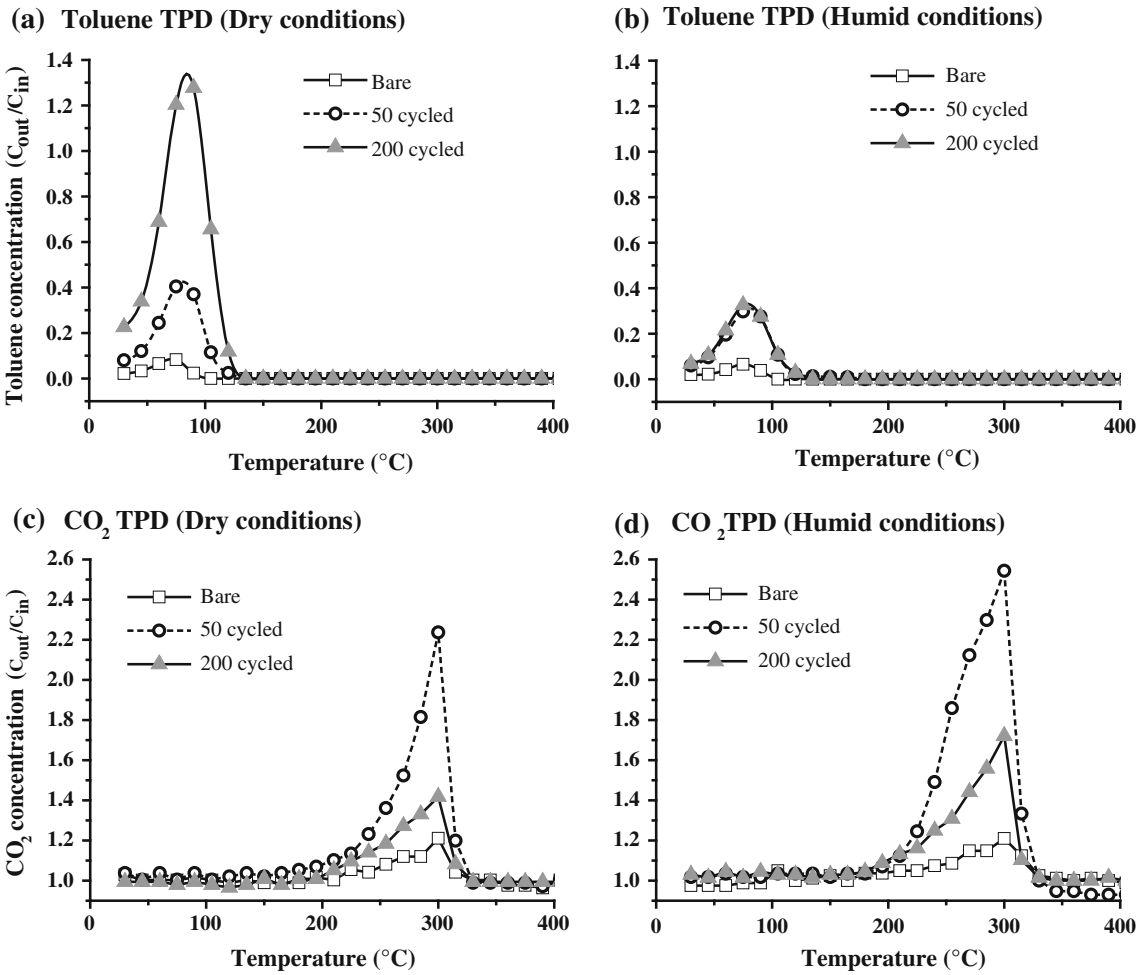

Fig. 4 Toluene and CO_2 TPD curves taken after toluene saturation under dry (**a**, **c**) and humid conditions (**b**, **d**) for bare silica and 50- and 200-cycle samples. **a** Toluene and **c** CO_2 TPD under dry conditions. **b** Toluene and **d** CO_2 TPD under humid conditions

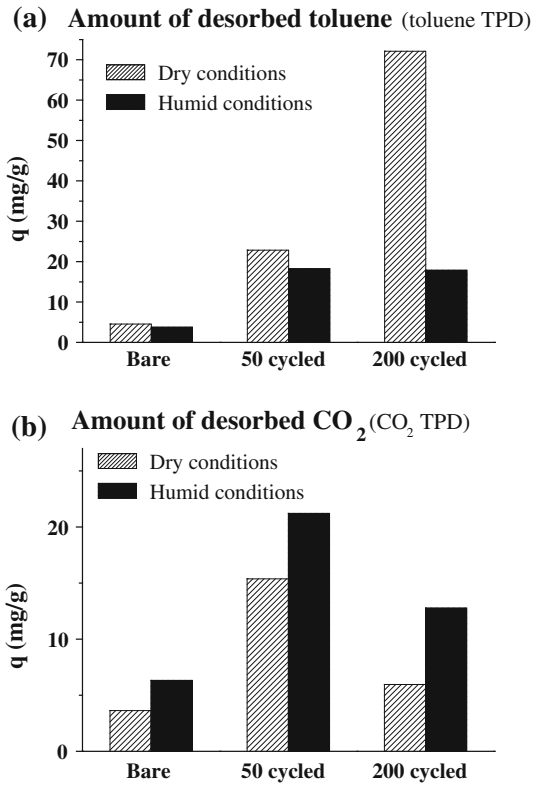

Fig. 5 Amounts of toluene (**a**) and CO_2 (mg/g) (**b**) desorbed from bare silica and 50- and 200-cycle samples. Results obtained after toluene saturation under dry and humid conditions

identified in the GC spectra. In all samples, toluene desorption was identified by a single, symmetric peak at 75 °C (Fig. 3a, b). CO_2 desorption had a maximum desorption peak at >250 °C (Fig. 3c, d). CO_2 production could be attributed to total oxidation of toluene on the sample surface during TPD (Choudhary and Mantri 2000). Figure 5 summarizes the integrated peak areas in toluene and CO_2 TPD curves from surfaces of all three samples saturated under dry and humid conditions.

Under dry conditions, the amount of desorbed toluene increased with the TiO_2 film thickness, which agrees with the toluene adsorption result in Fig. 3. Under humid conditions, the TPD profiles were much different (Fig. 5). Humidity significantly decreased the amount of toluene desorbed from all three samples compared to toluene desorption under dry conditions. This result agrees with the shorter breakthrough time and the roll-up curves in humid conditions (Fig. 3). Decreased toluene desorption after saturation in humid conditions was much more pronounced as the number of ALD cycles increased (from 0 to 200 cycles). However, both TiO_2/silica samples (50- and 200-cycle samples) had higher toluene desorption peaks under humid conditions than bare silica.

Under dry conditions, an asymmetric CO_2 desorption peak was centered at 300 °C for all three samples (bare silica and 50- and 200-cycle samples), and the 50-cycle sample had the largest CO_2 desorption peak. The CO_2 desorption for the bare silica sample saturated in the presence of water vapor did not change much, whereas CO_2 desorption peak intensities increased for both the 50- and 200-cycle samples. An additional desorption state centered at 250 °C also appeared when water vapor was added to TiO_2-covered samples. This lower-temperature desorption state of CO_2 can be attributed to carbon on the surface being oxidized by water adsorbed on the surface. Similar to dry conditions, under humid conditions the 50-cycle sample had the highest CO_2 desorption peak.

Given that the 50-cycle sample had pronounced Si 2p peaks, which completely disappeared in the 200-cycle sample, the surface of the 50-cycle sample probably consisted of both silica and TiO_2 sites, whereas 200-cycle sample was fully covered by TiO_2 (Dey et al. 2011). The higher reactivity of the 50-cycle sample towards total toluene oxidation than bare silica and the 200-cycle sample is probably related to the SiO_2/TiO_2 interfaces at the edges of TiO_2 grains. For example, under humid conditions, dissociative adsorption of water molecules could be facilitated at structural defects, such as steps, kinks, and Ti–Si interfaces, leading to an increased concentration of surface –OH groups. The high concentration of surface –OH group could aid in toluene oxidation at elevated temperature; thermal oxidation of toluene might be initiated and proceed by H or CH_3 abstraction due to interactions with oxygen atoms and OH radicals yielding benzyl (Dagaut et al. 2002). Under dry conditions, also, these interface sites could facilitates dissociative chemisorptions of oxygen, resulting in high oxidation reactivity for toluene.

4 Conclusion

We prepared thin TiO_2 films on silica with a mean pore size of 15 nm. Upon TiO_2 growth, the porous surface structure of the substrate was maintained. TiO_2-coated samples adsorbed more toluene than bare silica under dry conditions. Under humid conditions, displacement of adsorbed toluene by water was more pronounced for TiO_2-coated silica than bare silica. In the TPD experiments, CO_2 desorption from silica partially covered by TiO_2 (50-cycle samples) was much larger than desorption from bare and fully covered (200-cycle samples) silica films. These results suggest that TiO_2 deposition can be controlled using ALD to provide porous materials with a variety of chemical properties, which can be important for synthesizing adsorbents and catalysts to remove environmental pollutants.

Acknowledgments This work was supported by the National Research Foundation of Korea (NRF) Grant funded by the Korea government (MEST) (2012R1A1B3000992).

References

Avila, M.A.S., Breiter, R.: Competitive sorption of *cis*-DCE and TCE in silica gel as a model porous mineral solid. Chemosphere **72**, 1807–1815 (2008)

Chiang, Y.-C., Chiang, P.-C., Huang, C.-P.: Effects of pore structure and temperature on VOC adsorption on activated carbon. Carbon **39**, 523–534 (2001)

Ching-Huei, W.: Al_2O_3-supported transition-metal oxide catalysts for catalytic incineration of toluene. Chemosphere **55**, 11–17 (2004)

Choudhary, V.R., Mantri, K.: Temperature programmed desorption of toluene, *p*-xylene, mesitylene and naphthalene on mesoporous high silica MCM-41 for characterizing its surface properties and measuring heats of adsorption. Microporous Mesoporous Mater. **40**, 127–133 (2000)

Dagaut, P., Pengloan, G., Ristori, A.: Oxidation, ignition and combustion of toluene: experimental and detailed chemical kinetic modeling. Phys. Chem. Chem. Phys. **4**, 1846–1854 (2002)

Dey, N.K., Kim, M.J., Kim, K.D., Seo, H.O., Kim, D.W., Kim, Y.D., Lim, D.C., Lee, K.H.: Adsorption and photocatalytic degradation of methylene blue over TiO_2 films on carbon fiber prepared by atomic layer deposition. J. Mol. Catal. A **337**, 33–38 (2011)

Detavernier, D., Dendooven, J., Sree, S.P., Ludwigc, K.F., Martens, J.A.: Tailoring nanoporous materials by atomic layer deposition. Chem. Soc. Rev. **40**, 5242–5253 (2011)

Everaert, K., Baeyens, J.: Catalytic combustion of volatile organic compounds. J. Hazard. Mater. **109**, 113–139 (2004)

Foster, K.L., Fuerman, R.G., Economy, J., Larson, S.M., Rood, M.J.: Adsorption characteristics of trace volatile organic compounds in gas streams onto activated carbon fibers. Chem. Mater. **4**, 1068–1073 (1992). doi:10.1021/cm00023a026

Galli, S., Masciocchi, N., Colombo, V., Maspero, A., Palmisano, G., Lopez-Garzon, F.J., Domingo-Garcia, M., Fernandez-Morales, I., Barea, E., Navarro, J.A.R.: Adsorption of harmful organic vapors by flexible hydrophobic bis-pyrazolate based MOFs. Chem. Mater. **22**, 1664–1672 (2010). doi:10.1021/cm902899t

Heinen, A.W., Peters, J.A., Bekkum, H.V.: Competitive adsorption of water and toluene on modified activated carbon supports. Appl. Catal. A Gen. **194–195**, 193–202 (2000)

Henderson, M.A.: An HREELS and TPD study of water on TiO_2(110): the extent of molecular versus dissociative adsorption. Surf. Sci. **355**, 151–166 (1996). doi:10.1016/0039-6028(95)01357-1

Kim, H.S., Kim, T.W., Koh, H.L., Lee, S.H., Min, B.R.: Complete benzene oxidation over Pt–Pd bimetal catalyst supported on γ-alumina: influence of Pt–Pd ratio on the catalytic activity. Appl. Catal. A Gen. **280**, 125–131 (2005)

Kim, K.-J., Ahn, H.-G.: The adsorption and desorption characteristics of a binary component system of toluene and methylethylketone on activated carbon modified with phosphoric acid. Carbon **48**, 2198–2202 (2010)

Liotta, L.F.: Catalytic oxidation of volatile organic compounds on supported noble metals. Appl. Catal. B Environ. **100**, 403–412 (2010)

Lee, H.J., Seo, H.O., Kim, D.W., Kim, K.-D., Luo, Y., Lim, D.C., Ju, H., Kim, J.W., Lee, J., Kim, Y.D.: A high-performing nanostructured TiO_2 filter for volatile organic compounds using atomic layer deposition. Chem. Commun. **47**, 5605–5607 (2011)

Lee, J.W., Lee, J.W., Shim, W.G., Suh, S.H., Moon, H.: Adsorption of chlorinated volatile organic compounds on MCM-48. J. Chem. Eng. Data **48**, 381–387 (2003). doi:10.1021/je020158u

Li, L., Liu, S., Liu, J.: Surface modification of coconut shell based activated carbon for the improvement of hydrophobic VOC removal. J. Hazard. Mater. **192**, 683–690 (2011)

Nouri, S., Haghseresht, F.: Adsorption of *p*-nitrophenol in untreated and treated activated carbon. Adsorption **10**, 79–86 (2004). doi:10.1023/b:adso.0000024037.31407.15

Papaefthimiou, P., Ioannides, T., Verykios, X.E.: VOC removal: investigation of ethylacetate oxidation over supported Pt catalysts. Catal. Today **54**, 81–92 (1999)

Pires, J., Carvalho, A., de Carvalho, M.B.: Adsorption of volatile organic compounds in Y zeolites and pillared clays. Microporous Mesoporous Mater. **43**, 277–287 (2001)

Ruiz, J., Bilbao, R., Murillo, M.B.: Adsorption of different VOC onto soil minerals from gas phase: influence of mineral, type of VOC, and air humidity. Environ. Sci. Technol. **32**, 1079–1084 (1998). doi:10.1021/es9704996

Russo, P., Ribeiro Carrott, M., Carrott, P.: Adsorption of toluene, methylcyclohexane and neopentane on silica MCM-41. Adsorption **14**, 367–375 (2008). doi:10.1007/s10450-007-9099-0

Saqer, S.M., Kondarides, D.I., Verykios, X.E.: Catalytic oxidation of toluene over binary mixtures of copper, manganese and cerium oxides supported on γ-Al_2O_3. Appl. Catal. B Environ. **103**, 275–286 (2011)

Sayari, A., Hamoudi, S., Yang, Y.: Applications of pore-expanded mesoporous silica. 1. Removal of heavy metal cations and organic pollutants from wastewater. Chem. Mater **17**, 212–216 (2004). doi:10.1021/cm048393e

Scire, S., Minico, S., Crisafulli, C.: Pt catalysts supported on H-type zeolites for the catalytic combustion of chlorobenzene. Appl. Catal. B Environ. **45**, 117–125 (2003)

Sinha, A.K., Suzuki, K.: Three-dimensional mesoporous chromium oxide: a highly efficient material for the elimination of volatile organic compounds. Angew. Chem. Int. Ed. **44**, 271–273 (2005). doi:10.1002/anie.200461284

Sneh, O., Cameron, M.A., George, S.M.: Adsorption and desorption kinetics of H_2O on a fully hydroxylated SiO_2 surface. Sur. Sci. **364**, 61–78 (1996). doi:10.1016/0039-6028(96)00592-4

Spivey, J.J.: Complete catalytic oxidation of volatile organics. Ind. Eng. Chem. Res. **26**, 2165–2180 (1987). doi:10.1021/ie00071a001

Tidahy, H.L., Siffert, S., Lamonier, J.F., Zhilinskaya, E.A., Aboukais, A., Yuan, Z.Y., Vantomme, A., Su, B.L., Canet, X., De Weireld, G., Frere, M., N'Guyen, T.B., Giraudon, J.M., Leclercq, G.: New Pd/hierarchical macro–mesoporous ZrO_2, TiO_2 and ZrO_2–TiO_2 catalysts for VOCs total oxidation. Appl. Catal. A Gen. **310**, 61–69 (2006)

Tidahy, H.L., Siffert, S., Wyrwalski, F., Lamonier, J.F., Aboukais, A.: Catalytic activity of copper and palladium based catalysts for toluene total oxidation. Catal. Today **119**, 317–320 (2007)

Tsou, J., Magnoux, P., Guisnet, M., Orfao, J.J.M., Figueiredo, J.L.: Catalytic oxidation of volatile organic compounds: oxidation of methyl-isobutyl-ketone over Pt/zeolite catalysts. Appl. Catal. B Environ. **57**, 117–123 (2005)

Vichi, F.M., Tejedor–Tejedor, M.I., Anderson, M.A.: Effect of pore-wall chemistry on proton conductivity in mesoporous titanium dioxide. Chem. Mater. **12**, 1762–1770 (2000). doi:10.1021/cm9907460

Vildozo, D., Portela, R., Ferronato, C., Chovelon, J.-M.: Photocatalytic oxidation of 2-propanol/toluene binary mixtures at indoor air concentration levels. Appl. Catal. B Environ. **107**, 347–354 (2011)

Yang, C., Kaipa, U., Mather, Q.Z., Wang, X., Nesterov, V., Venero, A.F., Omary, M.A.: Fluorous metal-organic frameworks with superior adsorption and hydrophobic properties toward oil spill cleanup and hydrocarbon storage. J. Am. Chem. Soc. **133**, 18094–18097 (2011). doi:10.1021/ja208408n